Available online at www.sciencedirect.com
ScienceDirect
Quaternary Research 69 (2008) 377–387
QUATERNARY RESEARCH
www.elsevier.com/locate/yqres

# Geochronology of *Ailuropoda–Stegodon* fauna and *Gigantopithecus* in Guangxi Province, southern China

W.J. Rink [a,*], W. Wei [b], D. Bekken [c], H.L. Jones [a]

[a] *School of Geography and Earth Sciences, McMaster University, 1280 Main St. W., Hamilton, Ontario, Canada L8S 4K1*
[b] *Natural History Museum of Guangxi Zhuang Autonomous Region, Nannin, 530012, People's Republic of China*
[c] *Department of Anthroplogy, Field Museum of Natural History, Roosevelt Road at Lake Shore Drive, Chicago, Illinois 60605-2496, USA*

Received 15 December 2007
Available online 28 April 2008

**Abstract**

Pleistocene faunas from south China are difficult to subdivide based on the long temporal ranges of many taxa and a reduced number of genera in comparison to faunas from temperate north China. In south China, the *Ailuropoda–Stegodon* fauna is a very general one and includes a relatively stable suite of genera that apparently persisted for long periods of time. These attributes have made constraining its time range difficult. Application of electron spin resonance (ESR) dating of tooth enamel constrains the ages well where uranium uptake was minor. Where uranium uptake into teeth was significant, an approach combining ESR and $^{230}Th/^{234}U$ isotopic analysis also yields excellent ages. Previous estimates of early, middle and late Pleistocene time ranges previously determined by biostratigraphic seriation for the *Ailuropoda–Stegodon* fauna are confirmed in all cases but are made more precise with our approach, including specific time ranges for certain archaic taxa. Absolute dating also yields an extended time range for *Gigantopithecus blacki* of 1200 to 310 ka.


*Keywords:* Electron spin resonance dating; Tooth enamel; Uranium series dating; *Ailuropoda–Stegodon*; *Gigantopithecus*; Mammals

## Introduction

East Asia during the Pleistocene was home to diverse suites of distinctive mammalian taxa that are broadly distributed across a geologically and climatologically dynamic environment. Quaternary mammalian faunas in China can be seen to become more modern throughout the Pleistocene as surviving Tertiary forms are lost and modern taxa appear (see, for example, Dong et al., 2000; Louys et al., 2007). Geographically, this occurs throughout the region, but by the late early Pleistocene the progressive uplift of the Qingling mountains created an effective barrier to migration that separated the northern, Palearctic faunas from southern, Oriental faunas (Xue and Zhang, 1991). In north China this included suites of taxa such as the early Pleistocene *Proboscidipparion–Equus* fauna of the Nihewan basin, followed by the middle Pleistocene *Sinanthropus (Homo erectus)–Megaloceros pachyosteus* fauna from sites such as Zhoukoudian (Han and Xu, 1985). Pleistocene faunas from south China are characterized by subtropical and tropical taxa that, in many cases, are difficult to subdivide based on the long temporal ranges of many taxa and a reduced number of genera in comparison to faunas from temperate north China (Xue and Zhang, 1991). In south China the *Ailuropoda–Stegodon* fauna included a relatively stable suite of genera that persisted for long periods of time (Han and Xu, 1985, 1989). The *Ailuropoda–Stegodon* faunal suite is a very general one, however, and it has been difficult to determine reliable age estimates for many of the cave sites from which the faunas derive (Wang et al., 2007). In addition, the lack of reliable age data combined with the stratigraphic complexities of karstic cave sediments have prevented a more fine-grained understanding of the temporal characteristics of species level changes in local sequences as well as

* Corresponding author.
*E-mail address:* rinkwj@mcmaster.ca (W.J. Rink).

0033-5894/$ - see front matter © 2008 University of Washington. All rights reserved.
doi:10.1016/j.yqres.2008.02.008

Table 1
Summary of site characteristics

| Site | Latitude | Longitude | Biostratigraphic age | Elevation (a.m.s.l.) | Elevation (above local river level) |
|---|---|---|---|---|---|
| Wuyun | 23°35′ N | 106° 34′ E | Middle to late Pleistocene | 165 | 25 |
| Upper Pubu | 23°53.300′ N | 106° 59.167′ E | Middle to late Pleistocene | 155 | 15 |
| Wuming | 22°58.917′ N | 108° 13.544′ E | Middle Pleistocene | 152.5 | 21.5 |
| Daxin | 22′41.245′ N | 107° 14.026’ E | Middle Pleistocene | 360 | 110 |
| Liucheng | 24° 26.535′ N | 109° 12.512′ E | Early Pleistocene | 190 | 90 |

relationships between discrete geographic areas (Tong, 2005, 2006, 2007). Thus we aim to constrain the age of the faunal suite using radiometric methods.

Understanding the biostratigraphy of south China is important not only in regards to reconstructing the paleoenvironmental characteristics of this region but also for understanding Pleistocene climatic oscillation and the prevailing environmental context of local hominin species. It is also important for teasing apart the agents of Pleistocene megafaunal extinctions whether they be hominin exploitation, habitat alteration, sea level oscillations or some combination of several factors (e.g., Louys et al., 2007). In addition, greater temporal control contributes to studies of sympatric species (e.g., Saegusa, 2001) where differing ecological strategies are surmised.

Biostratigraphic sequences for Quaternary sites in China have historically been seriated based on presence or absence of Tertiary taxa, relative percentages between surviving archaic forms and modern taxa, and the presence or absence of a range of guide fossils within an assemblage. In addition, measurements of the sizes of individual elements are also important as several key groups can be shown to increase in size (e.g., the panda, genus *Ailuropoda*) throughout the Pleistocene (Xue and Zhang, 1991). Adding absolute dates further constrains and refines the temporal position of individual faunas.

The purpose of this paper is to constrain the temporal ranges of taxa within the *Ailuropoda–Stegodon* fauna, including *Gigantopithecus blacki*, which is known to occur in three of the five sites dated in this study. Table 1 shows that the cave sites occur at varying elevation, and Figure 1 shows the location of the sites.

This study provides absolute age determinations that further refine the temporal range of the associated taxa among the five sites by assuming that they correlate closely with dated samples drawn from the same stratigraphic levels. All of the deposits derive from silty and clay-rich breccias in karst caves that occur significantly above the level of the rivers in the valleys they face (Table 2).

Fluvial deposition (as floodplain runoff) is an important agent of accumulation for many karst cave faunas, and Zhang (1985) argues that fluvial deposition, along with carnivore hunting and porcupine collecting, is the most common mode of accumulation for three of the caves discussed here. We agree with Wang et al.’s (2007) hypothesis for the evolution of the cave systems in this area of Guangxi. They posit that over a long period of uplift and

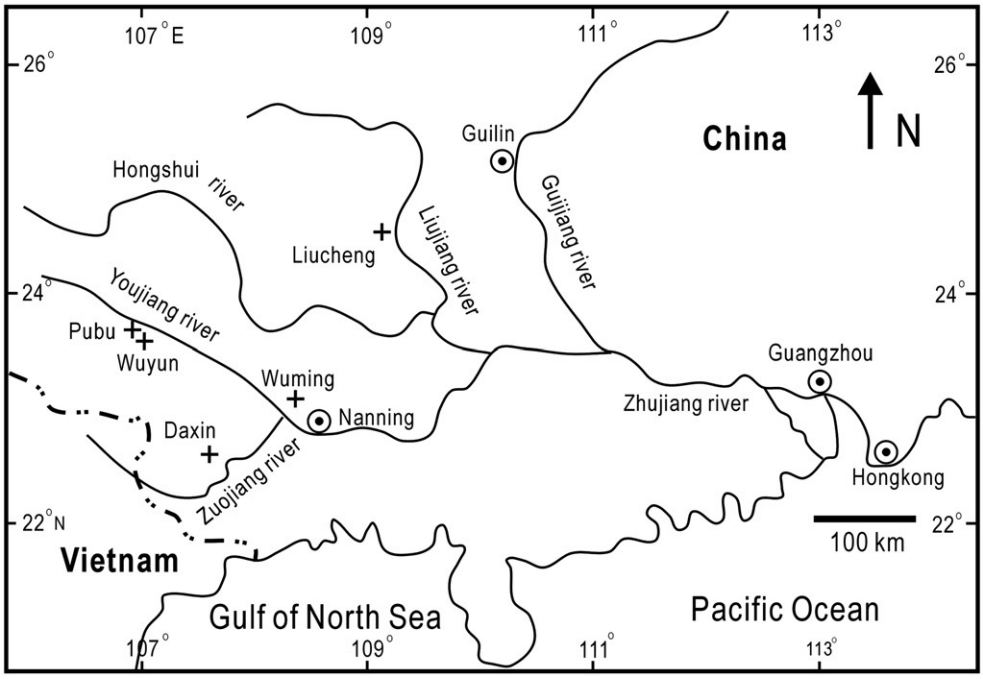


Figure 1. Map showing locations of study sites in Guangxi Province, China.

https://doi.org/10.1016/j.yqres.2008.02.008 Published online by Cambridge University Press

Table 2
Tooth sample identification and burial contexts

| McMaster sample # | Description |
|---|---|
| *Wuyun* | |
| WY1b | Rhino, from spherical back chamber, found in breccia of rounded pebbles that were light in colour, fluvial deposits. Approximately 1 m higher than WY 2. |
| WY2a | Pig, from spherical back chamber, among 3–5 cm limestone pebbles and cobbles of lighter colour. Also just below black organic layer. |
| WY3a | Caprine, from spherical back chamber, found in orange, fine grained sediment. |
| *Upper Pubu* | |
| PB1a | Unidentified fragment, in breccia. |
| PB2a | Unidentified fragment, in breccia, just below travertine. |
| PB3a | Unidentified fragment, in floor breccia, more than 30 cm from bedrock. |
| PB6a | Unidentified fragment, cemented into breccia below disturbed sediment. |
| *Daxin* | |
| DX2a | Caprine, in breccia chunk from floor of narrow channel. |
| DX2b | Caprine, in breccia chunk from floor of narrow channel. |
| DX3a | Primate, in breccia chunk from floor of narrow channel. |
| *Wuming* | |
| WM1a | Caprine, in breccia wall inside entrance 2, located above upper travertine which was about 20–25 cm thick. Tooth about 15 cm away from wall, backed by breccia. |
| *Liucheng* | |
| LC1b | Unidentified fragment, near entrance, found in upper breccia on wall between upper travertine and lower travertine, 5–10 cm from wall within breccia. |
| LC2a | Unidentified fragment, small travertine shelves in contact with tooth. |
| LC4a | Unidentified fragment, located up in nook in limestone. |
| LC5a | Unidentified fragment, taken from farther back in the cave, in breccia near excavation in fissure. |

river downcutting, limestone was dissolved and the caves were formed along paths of groundwater discharge at different elevations. During the end of each phase of cave development, sediments were introduced into the cavities through floodplain runoff and downward movement through openings in the limestone. From these considerations, one can view that the local elevation of the caves relative to present-day base level developed as basin groundwater descended to lower levels and the dissolution and sedimentary infilling of the caves followed as the river cut downward. Any actual uplift of the cave during this process relative to sea level would have been a result of regional and or local tectonic forces. The tectonic context of the sites shows that continuing uplift occurred in the region, associated with the flank of the uplift of the Tibetan Plateau to the west (Xue and Zhang, 1991). Thus, the present elevations of the caves will reflect a combination of erosion and downcutting as well as tectonic uplift (Guo and Shao, 1991). We believe that after reaching uplifted levels higher than floodstage of their local rivers, some upland (not fluvial) sediments could enter the caves from above, and it is likely at least some fauna were accumulated during these periods when the caves were not being regularly flooded and were relatively drier like they are today.

An important question addressed herein is the timing of the extinction of the giant ape *Gigantopithecus blackii*. The orangutan and *Gigantopithecus* share as a common ancestor the extinct primate *Sivapithecus*, and the latter is not believed to be associated directly with the evolution of the hominid line. (Ciochon et al., 1990). The genus *Sivapithecus* is known from the Miocene of Pakistan at about 8 Ma (Pilbeam, 1982). The genus *Gigantopithecus* is generally thought to have been present in south China from approximately 1.5 Ma to approximately 0.5 Ma; this genus is found in the Late Miocene in South Asia, but it is only known from the early through middle Pleistocene in China (Huang, 1979; Zhang, 1985; Huang et al., 1995). *Gigantopithecus blackii* is the only ape known to have become extinct in the Pleistocene, and as such is unique among the Old World Monkeys (Ciochon et al., 1990). At least seven localities are known from China, of which three are associated with lower Pleistocene faunas (Liucheng, Guangxi Province, Jianshi, Hubei Province and Wushan, Sichuan Province), and four are associated with middle Pleistocene faunas (Daxin, Wuming, Mohui and Bama, Guangxi Province) (Han and Xu, 1989; Xue and Zhang, 1991; Wang et al., 2005, 2007). Because of the apparent brief temporal range for *Gigantopithecus* in south China it is an important guide fossil; however, it is only known from isolated teeth and mandibles. As such we have aimed to constrain its age with radiometric methods within the *Ailuropoda–Stegodon* fauna, where relative ages have historically been, and are often still, only estimated through seriation of the presence or absence of Tertiary taxa.

There is variability in the composition of the fauna in each of the *Ailuropoda–Stegodon* assemblages we have dated. The taxonomic occurrence of the fauna at four of the five sites dated are listed in Table 3.

The Liucheng *Gigantopithecus* Cave site (Juyuandong) has long been recognized as an early Pleistocene faunal assemblage based on the presence of archaic taxa such as *Gomphotherium serridentoides*, *Nestoritherium praesinensis*, *Tapirus peii*, *Rhinoceros chiai*, *Dorcabune liuchengensis*, *Megalovis guangxiensis* and *Cervavitus* (*Cervoceros*) *fenqii* (Han and Xu, 1985).

At Daxin Cave, believed to be middle Pleistocene in age, three species are held in common with the earlier *Gigantopithecus* occurrence at Liucheng: *Pongo* sp., *Dicoryphochoerus ultimus*, and *Megalovis guangxiensis*, but none of these taxa occurs in the Wuming assemblage that also is dated to the middle Pleistocene. In addition, measurements of the *Gigantopithecus* dentition from Daxin and Wuming are larger than in the Liucheng series. Zhang (1985) argues that there is a general increase in tooth size from the early Pleistocene to the middle Pleistocene.

At Wuyun cave, the *Ailuropoda–Stegodon* assemblage occurs without *Gigantopithecus* and contains a number of small mammal taxa not found in the other assemblages discussed here but common to south China. These include insectivores such as *Neotetracus* cf. *sinensis*, bats such as *Hipposideros* sp. and *Scotomanes* sp., langurs (*Presbytis* sp.), and rodents such

https://doi.org/10.1016/j.yqres.2008.02.008 Published online by Cambridge University Press

Table 3
Taxonomic occurrence data for Wuyun, Daxin, Wuming, and Liucheng (Pei and Wu, 1956; Pei, 1957; Zhou, 1957; Han and Xu, 1985; Zhang, 1985; Xue and Zhang, 1991; Chen et al., 2002)

| Family | Common | Mammal | Wuyun | Daxin | Wuming | Liucheng |
|---|---|---|---|---|---|---|
| | Chinese alligator | *Alligator* cf. *sinensis* Fauvel | x | | | |
| Insectivora | | | | | | |
| | Shrew gymnure | *Neotetracus cf. sinensis* Trouessart | x | | | |
| | Himalayan shrews | *Soriculus* sp. | x | | | |
| | White-toothed shrews | *Crocidura* sp. | x | | | |
| | Mole shrews | *Anourosorex* sp. | x | | | |
| Chiroptera | | | | | | |
| | Roundleaf bats | *Hipposideros* sp. | x | | | |
| | Harelquin bats | *?Scotomanes* sp. | x | | | |
| Primates | | | | | | |
| | Macaque | *Macaca* sp. | x | x | x | |
| | Leaf monkeys | *Presbytis* sp. 1 | x | | | |
| | | *Presbytis* sp. 2 | x | | | |
| | Snub-nosed monkeys | *Rhinopithecus* sp. | | x | | |
| | | *Gigantopithecus blacki* Koenigswald | | x | x | x |
| | Gibbon | *Hylobates* sp. | | x | | |
| | Orangutans | *Pongo pygmaeus weidenreichi* Hooijer | x | | | |
| | | *Pongo* sp. | | x | | x |
| Rodentia | | | | | | |
| | Squirrels | *Callosciurus* sp. | x | | | |
| | | *Sciurotamias* sp. | x | | | |
| | Flying squirrel | *Belomys* sp. | x | | | |
| | Bamboo rat | *Rhizomys* sp. | | | x | |
| | Marmoset rat | *Hapalomys delacouri* Thomas | x | | | |
| | | *Leopoldamys* sp. | x | | | |
| | White-bellied rats | *Niviventer* sp. 1 | x | | | |
| | | *Niviventer* sp. 2 | x | | | |
| | | *Niviventer* sp. 3 | x | | | |
| | Old World rats | *Rattus* sp. | x | | | |
| | | *Rattus* cf. *edwardsi* Thomas | | | x | |
| | | *Rattus rattus* (Linnaeus) | | x | | |
| | Shrewmouse | *Mus* cf. *pahari* Thomas | x | | | |
| | Pencil-tailed tree mice | *Chiropodomys* cf. *gliroides* Allen | x | | | |
| | Chinese pygmy dormouse | *Typhlomys cinereus* Milne–Edwards | x | | | |
| | Brush-tailed porcupine | *Atherurus* cf. *macrourus* Linnaeus | x | | | |
| | | *Atherurus* sp. | | x | | x |
| | Crested porcupines | *Hystrix magna* Pei | | | | x |
| | | *Hystrix* cf. *subcristata* | | | x | |
| | | *Hystrix subcristata* Swinhoe | x | x | | x |
| Carnivora | | | | | | |
| | Dhole | *Cuon dubius* Teilhard | | | | x |
| | | *Cuon javanicus* (Matthew et Granger) | | x | | |
| | | *Cuon* cf. *javanicus antiquus* (Matthew et Granger) | x | | | |
| | Bear | *Ursus* sp. | | | x | |
| | Asiatic black bear | *Ursus thibetanus* Cuvier | x | x | | |
| | Asiatic black bear | *Ursus* cf. *thibetanus* Cuvier | | | | x |
| | Panda | *Ailuropoda melanoleuca baconi* Woodward | x | | | |
| | | *Ailuropoda melanoleuca fovealis* (Matthew et Granger) | | x | x | |
| | | *Ailuropoda microta* Pei | | | | x |
| | Hog badger | *Arctonyx collaris* Cuvier | x | x | | |
| | | *Arctonyx minor* Pei | | | | x |
| | Otter | *Lutra* sp. | | | x | |
| | Lesser oriental civet | *Viverricula malaccensis* (Gmelin) | | x | | |
| | | *Viverricula malaccensis fossilis* Pei | | x | | |
| | Civet | *Viverra* sp. | | | | x |
| | Palm civet | *Paradoxurus* sp. | x | | | |
| | Masked palm civet | *Paguma larvata* Hamilton–Smith | | x | | x |
| | Short-faced hyena | *Hyaena brevirostris licenti* Pei | | | | x |
| | Hyena | *Hyaena* sp. | | | x | |
| | Cat | *Felis sp.* | | | | x |
| | | *Felis teilhardi* Pei | x | | | x |
| | | *Felis (Panthera) pardus* (Linnaeus) | x | | | x |

https://doi.org/10.1016/j.yqres.2008.02.008 Published online by Cambridge University Press

Table 3 (*continued*)

| Family | Common | Mammal | Wuyun | Daxin | Wuming | Liucheng |
|---|---|---|---|---|---|---|
| Carnivora | | | | | | |
| | Tiger | *Felis tigris* Linnaeus | x | | | |
| | Hunting leopard | *Cynailurus pleistocaenicus* Zdansky | | | | x |
| Proboscidea | | | | | | |
| | | *Gomphotherium serridentoides* Pei | | | | x |
| | | *Stegodon* sp. | | | x | |
| | | *Stegodon preorientalis* Young | | | | x |
| | | *Stegodon orientalis* Owen | x | x | | |
| | Indian elephant | *Elephas maximus* Linnaeus | x | | | |
| Perissodactyla | | | | | | |
| | Horse | *Equus yunnanensis* Colbert | | | | x |
| | Kulan | *Equus hemionus* | | | | |
| | | *Nestoritherium praesinensis* Li | | | | x |
| | | *Megatapirus augustus* (Mathew et Granger) | x | x | | |
| | Tapirs | *Tapirus sinensis* Owen | x | | | |
| | | *Tapirus peii* Li | | | | x |
| | Rhinoceros | *Rhinoceros chiai* Li | | | | x |
| | | *Rhinoceros sinensis* Owen | x | x | x | |
| Artiodactyla | | | | | | |
| | Suid | *Suidae* | | | | x |
| | | *Dicoryphochoerus ultimus* Han | | x | | x |
| | Pigs | *Sus* sp. | | x | x | |
| | | *Sus australis* | | | | x |
| | | *Sus bijiashanensis* Han, Xu et Yi | | x | x | |
| | | *Sus liuchengensis* | | | | x |
| | | *Sus peii* Han | | | | x |
| | | *Sus xiaozhu* Han, Xu et Yi | | | | x |
| | Boar | *Sus scrofa* Linnaeus | x | | | |
| | Boar | *Sus scrofa* | | | x | |
| | | *Potamochoerus nodosarius* | | | | x |
| | | *Dorcabune liuchengensis* Han | | | | x |
| | Muntjac | *Muntiacus* sp. | x | x | | |
| | Muntjac | *Muntiacus lacustris* Teilhard et Trassaert | | | | x |
| | | *Cervocerus* (*Cervavitus*) *fenqii* Han | | | | x |
| | Rusa deer | *Rusa yunnanensis* Li, Pan et Lu | | | | x |
| | Deer | *Cervus* sp. indet. 1 | x | x | | |
| | Deer | *Cervus* sp. indet. 2 | x | | | |
| | | *Bovinae* gen. et sp. indet. | x | | x | |
| | | *Bibos* sp. | | x | | x |
| | | *Caprinae* gen. et sp. indet. | | x | | x |
| | Serows | *Capricornis sumatraensis* Bechstein | x | | | |
| | | *Capricornis* cf. *sumatraensis* Bechstein | | | x | |
| | | *Megalovis guangxiensis* Han | | x | | x |

as *Belomys* sp., *Leopoldamys* sp., and *Hapalomys delacouri* (Table 2). The Wuyun assemblage dates to the middle to late Pleistocene and has few remaining archaic taxa but includes *Megatapirus augustus*. Two species of proboscideans are found in association, the archaic *Stegodon orientalis* and modern *Elephas maximus,* indicating a potential early late Pleistocene age for this assemblage (Chen et al., 2002). Previous dating of flowstones using uranium series dating (Wang et al., 2007) indicate the the excavated fossiliferous assemblages dates to between 21,111+/−390 yr ago and 356,390+/−29,000 yr ago. These dates are consistent with previous biostratigraphic age evaluations of middle to late Pleistocene (Chen et al., 2002).

Taxonomic data is currently unavailable for the Upper Pubu Cave. However, an extensive faunal list does exist for the Lower Pubu Cave (Wang et al., 2007). These fauna have been dated on biostratigraphic grounds to a time range of late middle Pleistocene to late Pleistocene. Since our samples come from a cave 10 m directly above the Lower Pubu Cave in the same karst remnant, they come from an older cave system than Lower Pubu based on our understanding of cave formation in this region.

Electron spin resonance (ESR) is a radiometric dating technique that is based on the effects of natural radioactivity on the atomic-scale defects in a mineral (Rink, 1997). Tooth enamel is carbonated hydroxyapatite: $Ca_5$ ($PO_4$, $CO_3$) (OH). Natural radiation converts $CO_3$ sites into radiation defects: $CO_3^{2-}$, which is paramagnetic and can be detected with ESR. At burial the concentration of $CO_3^{2-}$ defects begins to increase as a function of the emissions of alpha, beta and gamma radiation from the $^{238}U$, $^{235}U$, and $^{232}Th$ decay chains and from $^{40}K$ in the natural environment surrounding the buried tooth. It also grows due to cosmic radiation penetrating the earth's surface. In ideal burial conditions the age is given by the ratio of the total radiation dose

https://doi.org/10.1016/j.yqres.2008.02.008 Published online by Cambridge University Press

(palaeodose) to the annual radiation dose in the environment. The palaeodose is obtained by artificial irradiation of the enamel and ESR measurements. However, the annual dose sometimes also includes a contribution from uranium (U) absorbed from groundwater by the dental tissues over time.

The process of absorption of U into teeth is referred to as U uptake. The U uptake must either be modeled and included in the environmental annual dose, or directly accounted for by measurement of the concentrations of U and Th isotopes in the sample. Modeling of U uptake is usually accomplished using two simple assumptions: 1) the U in the dental tissues is assumed to have accumulated instantaneously after burial; this model is called early uptake (EU), or 2) the U found at the time of collection is assumed to have increased in equal increments in each yr of the burial; this model is called linear uptake (LU). This approach yields two ESR ages for a single sample called the EU and LU model ages. However it is also possible for the U to be accumulated late in the burial history, therefore a limiting case can be obtained called the recent or late uptake model. It provides a maximum burial age.

The analysis of uranium and thorium isotopes in dental tissues allows a much better determination of U uptake history because the radioactive decay of all $^{238}U$ and $^{234}U$ in the sample leads to the production of $^{230}Th$. The ratios among these isotopes can then be used to calculate a more accurate U uptake model (Grün et al., 1988). In this approach the rate of uranium uptake is modeled using a family of equations of the form:

$$U(t) = U_0[t/T]^{p+1} \quad (1)$$

where:

U is the uranium concentration at any time
$U_0$ is the initial uranium concentration
$t$ is the time
$T$ is the total burial time (age of the sample)
and $p$ is a numerical value that can range from −1 to large positive values.

Various values of $p$ and $t$ are compared to the total dose absorbed into the enamel to evolve a specific uptake model. It is constrained by the uranium and thorium isotopic values to obtain a value for $p$ in each tissue at a unique time $T$ (burial age) that is consistent with the total enamel dose as measured by ESR plus the calculated additional dose rates from sediments and cosmic rays not associated with uranium uptake.

Evolved $p$ values correspond to a potential continuum of uptake models

| Model | $p$ value |
|---|---|
| Early Uptake (EU) | −1 to 0 |
| Linear Uptake (LU) | near 0 |
| Recent (or late) Uptake | >0 |

The combination of the ESR and isotopic results yields coupled ESR/$^{230}Th$/$^{234}U$ age estimates that can be considered as a reasonably accurate burial age. ESR ages calculated without U and Th isotopic analysis are special cases of equation (1) where EU would correspond to $p=-1$ and LU would correspond to $p=0$.

In ideal dating situations, a number of teeth spanning the thickness of the sedimentary deposit are dated to establish the time range of a deposit. In our sites we were limited to determination of the age of the deposit using only the samples that could be found in the surface of the breccias, often in thin parts remaining on the cave wall. This is because in most of the caves nearly all of the deposit had been removed by previous excavators. However, this approach was much better than trying to use museum samples whose radiation dose environment could not likely be confidently reconstructed. As a result of these constraints, our samples do not come from enough locations to span the entire thickness of sediments in which faunal elements were recovered in earlier excavations. Here we relate the ages of various faunal elements found in the cave sequence by assuming that they correlate closely with dated samples drawn from the same stratigraphic levels. Table 2 gives the relevant information about the find locations within each sequence.

## Methods and sample collection

Samples were collected by inspecting the small patches of remaining breccia on cave walls and removing sediment and nearby cave-wall limestone or travertine along with the mammal teeth (many were fragmentary and taxonomic identification was not possible). The characteristics of each recovered sample are found in Table 2. In-situ radiation dosimetry was carried out in a few locations for comparison with dose rates determined using attached sediment and limestone chemical analyses, though chemical analyses of the sediment and nearby limestone were used for reconstructing the gamma dose rates using published dose rate conversion data (Adamiec and Aitken, 1998).

Sediments such as breccias, which are often found to host fossils in limestone caves, are generally composed of at least two different materials, such as clay and limestone, that have significantly different gamma radioactivity levels. This gives rise to a distribution of gamma dose rates in thick packages (>approx. 1 m thick) of such sediments that is characterized by both the range in particle sizes of the large elements and the relative amounts of radioactivity in each of the two materials (Brennan et al., 1997). Many of our samples came from thin layers of breccia, or simply a thin layer of the hard clay fraction of a breccia that was within 5 cm or so of the cave wall. Since the effects of gamma radioactivity are distributed over a sphere with a radius of about 30 cm, in these cases we assumed that half of the gamma dose rate came from the radioelements in the cave wall, and the other half from the radioelements in the thin layer of breccia or clay portion of breccia. In cases where we had thick breccia, we assumed that the radioelements in the sample collected near the tooth were representative of those in the breccia as a whole. In order to account for natural variability in the gamma dose rate due to the unknown distribution of radioactivity in the limestone vs. the clay fraction, we introduced a +/−20% error term in the gamma dose rate which was folded into the total error obtained on a given age estimate.

https://doi.org/10.1016/j.yqres.2008.02.008 Published online by Cambridge University Press

Table 4
Electron Spin Resonance Dating Analytical Data

| McMaster sample # or site | $D_E$ (Gy) | U en (ppm) | U den (ppm) | U sed (ppm) | K sed (wt %) | Th sed (ppm) | Enamel thickness (μm) | Sed side rem (μm) | Den side rem (μm) |
|---|---|---|---|---|---|---|---|---|---|
| *Wuyun* | | | | | | | | | |
| WY1b | 99.8±12.7 | 0.38 | 2.05 | 0.89 | 0.21 | 3.89 | 724±130 | 160±26 | 190±36 |
| WY2a | 120.2±10.7 | 0.38 | 1.26 | 0.46 | 0.51 | 11.99 | 636±80 | 93±17 | 99±19 |
| WY3a | 100.2±11.6 | n.d. | 2.75 | 1.46 | 0.31 | 4.79 | 807±136 | 217±40 | 232±45 |
| *Upper Pubu* | | | | | | | | | |
| PB1a | 207.7±42.9 | n.d. | 4.85 | 1.65 | 0.29 | 9.15 | 972±180 | 192±42 | 201±44 |
| PB2a | 170.3±15.3 | 0.19 | 6.98 | 2.48 | 0.55 | 14.52 | 1010±203 | 126±23 | 135±26 |
| PB3a | 244.2±36.9 | n.d. | 13.72 | 3.00 | 0.46 | 14.34 | 1521±151 | 211±46 | 227±52 |
| PB6a | 162.1±5.2 | 1.37 | 7.56 | 2.75 | 1.71 | 15.03 | 1084±93 | 98±10 | 120±16 |
| *Daxin* | | | | | | | | | |
| DX2a | 731.7±42.1 | 1.16 | 70.08 | 4.60 | 0.18 | 8.42 | 648±57 | 249±21 | 380±38 |
| DX2b | 728.7±28.8 | 0.11 | 65.87 | 4.60 | 0.18 | 8.42 | 525±50 | 275±23 | 406±40 |
| DX3a | 536.3±17.6 | 0.17 | 68.02 | 7.70 | 0.27 | 9.18 | 968±182 | 221±26 | 293±39 |
| *Wuming* | | | | | | | | | |
| WM1a | 511.3±49.7 | n.d. | 4.38 | 2.08 | 0.563 | 6.58 | 637±115 | 90±45 | 55±27 |
| *Liucheng* | | | | | | | | | |
| LC1b | 1541.2±85.0 | 1.99 | 34.58 | 6.04 | 0.37 | 5.87 | 1772±266 | 749±59 | 1167±115 |
| LC2a | 824.6±30.5 | 0.03 | 25.35 | 6.63 | 0.33 | 7.09 | 676±77 | 596±63 | 770±92 |
| LC4a | 685.0±36.4 | n.d. | 14.16 | 5.18 | 0.37 | 4.51 | 1207±100 | 912±121 | 1075±159 |
| LC5a | 699.3±28.4 | n.d. | 4.86 | 5.96 | 0.28 | 7.53 | 1578±297 | 1030±193 | 1085±198 |

$D_E$ is equivalent dose, U is uranium, K is potassium, Th is thorium, Sed is sediment, En is enamel, Den is dentine, Sed is sediment, Rem is removed, ppm is parts per million, wt % is weight percent, Gy is Gray, μm is micrometer, NA is not applicable. Errors in Th and K values range from±2–8% of the value and are not reported here. Errors in U values are±0.1 ppm, n.d. means not detected and value is less than 0.1 ppm. The equivalent dose (DE) values and their uncertainties were determined using the procedure of Brumby (1992). Eight to 10 aliquots of each sample were irradiated with exponentially spaced doses. The samples were irradiated using a 60 Co source at the McMaster Nuclear Reactor. A Bruker ER 100 X-band spectrometer was used to measure the ESR signals using the following conditions: modulation amplitude=0.5 mT, time constant=10.24 ms, scan time=0.48 MT/s and microwave power=2.0 mW. Uranium concentrations in dental tissues and sediment were determined using delayed neutron counting, and thorium and potassium concentrations in the sediment were determined using instrumental neutron activation analysis (INAA).

One unusual aspect of the environments we sampled is that it is likely that some of fossils we have dated were deposited by fluvial activity as the cave was exposed in the valley near the base level of the local river. Thus the moisture content in the sediment may have been episodically much higher than that typical of the sediments today (around 20% moisture). However, as the local uplift of the land, coupled with downcutting to lower local river base levels continued, the caves rose up, and later sedimentation and fossil deposition were associated with local sediments moving through openings in the roof of the cave and moving in at the front. The moisture content of these sediments would have been much more like that of today than of the sediments fluvially deposited in the very earliest stages of filling of the cave. Thus the use of the present-day moisture content is justified because it represents our best estimate of the moisture content over almost the entire history of the cave sediments. To account for changes in this value that are expected due to long term climatic fluctuations, we introduced an error term of +/−50% to the typical 20% moisture-content value, which was folded into the total error obtained on a given age estimate (the value used was 20%+/−10% moisture).

## Results

Uranium (U) accumulation in dental tissues was found to vary widely among the sites studied. The U concentrations in enamel and dentine range from <0.1 to 2.28 ppm and 5 to 33 ppm, respectively (Table 4).

For teeth with significant U concentrations this led to a wide spread in the early uptake (EU) and linear uptake (LU) model ages at Daxin and in LC1 and LC2 at Liucheng, while many teeth showed lower levels of U uptake, which made EU and LU ages statistically indistinguishable (all teeth at Wuyun, Upper Pubu, and Wuming and LC4 and LC5 at Liucheng) (Table 5). For teeth with statistically indistinguishable EU and LU model ages, we did not to do uranium and thorium isotopic analysis to try to further refine the uptake models, as it is not necessary.

Table 5
Mass spectrometric $^{230}Th/^{234}U$ dating results for enamel and dentine

| Sample | Uranium (ppm) | $^{230}Th/^{232}Th$ (±2σ) | $^{234}U/^{238}U$ (±2σ) | $^{230}Th/^{234}U$ (±2σ) |
|---|---|---|---|---|
| *Daxin* | | | | |
| DX3a Dentine | 64.23±0.14 | 3890±510 | 1.2197±0.0025 | 0.5717±0.0313 |
| *Liucheng* | | | | |
| LC1b Enamel | 2.28±0.004 | 2516±105 | 1.2048±0.0135 | 0.9669±0.0142 |
| LC1b Dentine | 3.17±0.2 | 1645±35 | 1.1210±0.0115 | 0.3949±0.0090 |
| LC2a Dentine | 24.03±0.09 | 379±20 | 1.1432±0.0067 | 0.2980±0.0139 |

All isotopic ratios are activity ratios. The preparation and measurement of samples for isotopic analysis follows the procedures described in Jones et al., 2004.

https://doi.org/10.1016/j.yqres.2008.02.008 Published online by Cambridge University Press

For selected teeth with significant U, mass spectrometric uranium and thorium isotopic analysis was done to provide burial ages by combination of the ESR data with the isotope analysis. The results of the isotopic analyses are given in Table 5. The coupled ESR/$^{230}$Th/$^{234}$U age estimates with corresponding *p*-values are given in Table 6.

Where uranium uptake was significant, the most reliable age estimates are those provided in the coupled ESR/$^{230}$Th/$^{234}$U age column of Table 6. This is because the isotopic data which they incorporate provides independent control on the uranium uptake in the tooth, circumventing the problem of assuming an uptake model such as early or linear uptake (EU or LU). (Grün et al., 1988). Good agreement was found for the two coupled ESR/$^{230}$Th/$^{234}$U ages at Liucheng of 973+111/−100 ka and 1082+113/−91 ka. The coupled age analyses show that the uptake histories of these two teeth were very different. Tooth LC1b showed *p* values of −0.54 in the enamel and 0 in the dentine, yielding uptake about midway between classical early and linear uptake values for the enamel and linear for the dentine. Tooth LC2a, on the other hand, showed strongly recent uptake with *p* values of 18.5. The coupled ESR/$^{230}$Th/$^{234}$U ages are also in excellent agreement with the range of EU and LU ages for the two teeth with small amounts of U uptake (LC4a and LC5a), clearly indicated by their classical EU and LU model ages being statistically indistinguishable. These were 912±121 ka (EU) to 1075±159 ka (LU) and 1030±193 ka (EU) and 1085±198 ka (LU) ka, respectively. On balance, the results for the four teeth point to a depositional age range (including all uncertainties) at Liucheng of about 1200 to 900 ka, confirming their early Pleistocene biostratigraphic age.

One tooth from Daxin yielded a coupled ESR/$^{230}$Th/$^{234}$U age of 340+40/−32 ka. It is a for a primate tooth that must be (based on

Table 6
Tooth enamel electron spin resonance dating results and coupled ESR/$^{230}$Th/$^{234}$U age estimates

| McMaster sample # or site | Gamma dose rate (μGy/a) | Cosmic dose rate (μGy/a) | EU,LU β sed dose rate μGy/yr | EU α en dose rate μGy/yr | EU β en dose rate μGy/yr | EU β den dose rate μGy/yr | EU total dose rate μGy/yr | LU α en dose rate μGy/yr | LU β en dose rate μGy/yr | LU β den dose rate μGy/yr | LU total dose rate μGy/yr | EU ESR model age (ka) | LU ESR model age (ka) | Coupled ESR/$^{230}$Th/$^{234}$U age (ka) | *p*-Value en | *p*-Value den |
|---|---|---|---|---|---|---|---|---|---|---|---|---|---|---|---|---|
| *Wuyun* | | | | | | | | | | | | | | | | |
| WY1b | 379 | 7 | 58 | 117 | 26 | 39 | 625 | 52 | 12 | 18 | 526 | 160±26 | 190±36 | | | |
| WY2a | 1030 | 7 | 119 | 95 | 21 | 23 | 1295 | 40 | 9 | 11 | 1216 | 93±17 | 99±19 | | | |
| WY3a | 324 | 7 | 75 | 0 | 0 | 52 | 458 | 0 | 0 | 24 | 430 | 219±41 | 233±46 | | | |
| *Upper Pubu* | | | | | | | | | | | | | | | | |
| PB1a | 861 | 60 | 75 | 0 | 0 | 80 | 1076 | 0 | 0 | 36 | 1032 | 193±42 | 201±45 | | | |
| PB2a | 1001 | 60 | 128 | 54 | 14 | 96 | 1355 | 23 | 6 | 44 | 1263 | 126±23 | 135±26 | | | |
| PB3a | 859 | 60 | 85 | 0 | 0 | 150 | 1153 | 0 | 0 | 69 | 1072 | 212±46 | 228±52 | | | |
| PB6a | 835 | 60 | 213 | 350 | 96 | 96 | 1650 | 157 | 45 | 46 | 1354 | 98±10 | 120±16 | | | |
| *Daxin* | | | | | | | | | | | | | | | | |
| DX2a | 746 | 38 | 167 | 427 | 90 | 1472 | 2940 | 207 | 44 | 723 | 1925 | 249±21 | 380±38 | | | |
| DX2b | 746 | 38 | 194 | 42 | 8 | 1626 | 2653 | 20 | 4 | 793 | 1795 | 275±23 | 406±40 | | | |
| DX3a | 1055 | 38 | 185 | 60 | 15 | 1076 | 2430 | 28 | 7 | 517 | 1830 | 221±26 | 293±39 | 340 + 40 −32 | | 0.91± 0.37 |
| *Wuming* | | | | | | | | | | | | | | | | |
| WM1a | 563 | 60 | 137 | 0 | 0 | 113 | 873 | 0 | 0 | 54 | 814 | 585± 104 | 628± 117 | | | |
| *Liucheng* | | | | | | | | | | | | | | | | |
| LC1b | 488 | 30 | 92 | 873 | 245 | 328 | 2058 | 426 | 120 | 162 | 1320 | 749±60 | 1167± 115 | 1042 + 164 −102 | −0.54± 0.12 | 0± 3.92 |
| LC2a | 529 | 30 | 218 | 0 | 0 | 591 | 1384 | 0 | 0 | 287 | 1064 | 602±64 | 775±93 | 1082 + 113 −91 | | 18.5± 4.12 |
| LC4a | 391 | 30 | 108 | 0 | 0 | 217 | 745 | 0 | 0 | 106 | 635 | 919± 123 | 1079± 161 | | | |
| LC5a | 498 | 30 | 84 | 0 | 0 | 61 | 673 | 0 | 0 | 30 | 642 | 1039± 196 | 1090± 199 | | | |

EU is early uptake model, LU is linear uptake model, β is beta, α is alpha, Cem is cementum, den is dentine, en is enamel, μm is micrometer ($1\times10^{-6}$ m), μGy/yr is $1\times10^{-6}$ Gy/yr. ESR dating was carried out according to standard protocols described in Rink et al. (1994) using the ROSY age determination software (Brennan et al., 1997) version 2.0. This program incorporates new calculations of beta attenuation based on one-group theory (O'Brien et al., 1964; Prestwich et al., 1997). Age uncertainties in ESR model ages are obtained in the Rosy software through determination of each individual model age twice: once with all input values at their minimum value (value minus the uncertainty) and the other value obtained by inputting each value plus its own uncertainty. The range between these estimates gives the actual error reported for each of the EU and LU ages for a single tooth. The coupled ESR/$^{230}$Th/$^{234}$U ages were calculated with the program DATA-WJR kindly provided by Dr. R. Grün of Australian National University. For the coupled ESR/$^{230}$Th/$^{234}$U ages, the reported uncertainties are calculated based on a quadrature sum of all the uncertainties in the input values in the DATA-WJR program.

https://doi.org/10.1016/j.yqres.2008.02.008 Published online by Cambridge University Press

Table 7
Best age estimates for faunal assemblages based on ESR model ages and or coupled ESR/$^{230}$Th/$^{234}$U ages

| Site | Faunal assemblage best age estimate (including error range) (ka) |
|---|---|
| Wuyun | 76–279 [a] |
| Upper Pubu | 88–280 [a] |
| Daxin | 308–380 [b] |
| Wuming | 481–745 [c] |
| Liucheng | 940–1206 [d] |

[a] Determined using the spread between the minimum EU and maximum LU ESR age results among several dated teeth. At these sites there was no statistical difference between EU and LU age results on individual teeth, thus the reported spread in results is not related to effects on the ages due to a large range in uranium uptake.

[b] Determined using the spread between the minimum and maximum coupled ESR/$^{230}$Th/$^{234}$U age (based on its uncertainty) on DX3a since it was the best dated among those studied; the other two samples yielded ESR EU and LU age estimates that were statistically indistinguishable from the coupled ESR/$^{230}$Th/$^{234}$U age on DX3a.

[c] Determined using the spread between minimum and maximum ESR EU and LU ages on the only dated sample, which had little uranium uptake leaving no statistical difference between the EU and LU ages.

[d] Determined using the spread between the minimum and maximum coupled ESR/$^{230}$Th/$^{234}$U ages (including uncertainty) of LC1b and LC2a since they were the best dated among those studied; the other samples were dated by ESR only.

the faunal lists) either an orangutan or *Pongo* sp., since *Gigantopithecus blacki* was ruled out by one of us in the field (WW). The *p* values of 0.91 show that the tooth experienced near linear to slightly recent uptake. This also agrees with the LU age range for the other two teeth from Daxin, which yielded ages of 275±23 (EU) to 406±40 (LU) ka and 221±26 (EU) to 293±39 (LU) ka, respectively, for caprid teeth. These results firmly place the depositional age of the fossils at Daxin at 300 to 370 ka, confirming their middle Pleistocene biostratigraphic age estimate.

A tooth from Wuming yielded statistically indistinguishable EU and LU model age estimates of 573±95 (EU) and 616±106 (LU) ka, due to the small amount of U uptake that occurred. The result was on a caprid tooth, not identified to species, but which is very likely *Capricornis sumatraensis* as that is the only caprid identified from Wuming to date. Considering all of the uncertainty in the age estimates, we obtain an age range of about 720 to 480 ka. This single age indicates the likelihood that the site predates the Daxin fossils and suggests an early middle Pleistocene age.

The Upper Pubu and Wuyun sites, located in close proximity to each other, both yielded age estimates that span the transition from middle to late Pleistocene, both cases hosting teeth with EU and LU age estimates ranging from about 270 ka (EU) to about 90 ka (LU). Due to the small amounts of uranium uptake the youngest elements in each site seem to indicate a clear late Pleistocene burial age for those teeth. Notably, WY1b was a rhinoceros tooth, very likely *Rhinoceros sinensis*, the only rhinoceros identified for the site; and WY3a was a caprid, very likely of *Capricornus sumatraensis*, the only caprid identified at Wuyun.

For teeth with statistically indistinguishable classical EU and LU ages, we chose not to do uranium and thorium isotopic analysis to further refine the uptake models, as it is difficult experimentally and unnecessary in any case. It is possible that the true burial ages of those teeth could be older because the possibility of recent uptake remains untested.

Table 7 provides a summary of the best age estimates for each of the sites studied. The ages are best constrained at Daxin and Liucheng, while larger ranges are required for conservative estimates (including all errors) for the three other sites. Liucheng dates to early Pleistocene, while Daxin and Wuming are middle Pleistocene. Wuyun and Upper Pubu provide age ranges that span middle to late Pleistocene.

## Discussion

The dating results allow the temporal range of selected fossil groups to be further refined in comparison with accepted biostratigraphic results. We stress that the results do not constrain the entire range for a given genus, only a range that is indicated by their presence at the sites in this study.

The *Ailuropoda–Stegodon* fauna of south China is present throughout the Pleistocene, and it is defined very broadly by the presence of a range of genera that includes *Macaca*, *Hystrix*, *Ailuropoda*, *Stegodon orientalis*, *Tapirus sinensis*, *Megatapirus*, *Rhinoceros sinensis*, and *Rusa* (Pei, 1957; Xue and Zhang, 1991). The individual taxa of the broadly defined *Ailuropoda–Stegodon* fauna change throughout the Pleistocene, however, and can be further subdivided when looking at early, middle and late Pleistocene-aged assemblages. Historically, the presence or absence of surviving Tertiary taxa was used to further delineate early, middle, and late Pleistocene occurrences (e.g., Xue and Zhang, 1991; Dong et al., 2000).

The assemblages discussed here can be dated to the early, middle, and late Pleistocene on biostratigraphic evidence. Biostratigraphic ages in general agree well with the absolute dates given above.

The site of Liucheng in Guangxi Zhuang Autonomous Region contains an important faunal assemblage that is the type sample for the *Ailuropoda–Stegodon* fauna (Pei, 1957). Excavated in 1956, it dates to the early Pleistocene, yielding here for the first time an absolute age of about 1000 ka for the type assemblage. It contains several late Tertiary taxa such as *Gomphotherium serridentoides*, *Nestoritherium praesinensis*, *Dorcabune liuchengensis*, and *Cervoceros fenqii*. It also contains early Pleistocene taxa such as *Cuon dubius*, *Hyena licenti*, *Felis teilhardi*, and *Equus yunnanensis* in addition to the abundant remains of *Gigantopithecus blacki* (Xue and Zhang, 1991; Zhou, 1957).

The Daxin and Wuming assemblages, both from cave excavations in Guangxi Zhuang Autonomous Region, date to the early middle Pleistocene (Pei and Wu, 1956). They contain typical members of the *Ailuropoda–Stegodon* fauna as well as guide fossils such as *Gigantopithecus blacki* in association with the orangutan, *Pongo* sp., that comes into the region during the middle Pleistocene (Xue and Zhang, 1991). Daxin was discovered in 1956, while Wuming was excavated in 1962 (Wu and Lin, 1985). The dating results provide a timeline to the increase in size of *Gigantopithecus blacki* teeth from the early to the early middle Pleistocene, which was previously only known to span the time from early to middle Pleistocene.

The new dates for three *Gigantopithecus* localities further constrains the temporal range for this taxon in China. These dates agree well with the general observation that *Gigantopithecus* is

https://doi.org/10.1016/j.yqres.2008.02.008 Published online by Cambridge University Press

present in China during the early to middle Pleistocene, and the ages for Liucheng predate the age of more southerly occurrences of *Gigantopithecus* such as at Tham Khuyen Cave, Vietnam, dated to 475±125 ka, where *Homo erectus* remains were also found (Ciochon et al., 1996). *Gigantopithecus* is found in association with hominid fossils at three locations in China and one in Vietnam. In China, these sites are Jianshi in Hubei Province (Gao, 1975; Zhang, 1985), Wushan (Longgupo Cave) in Sichuan Province (Huang and Fang, 1991; Huang et al., 1995) and Mohui cave in Guangxi Province (Wang et al., 2005, 2007). U-Series dating results at Mohui Cave indicate co-occurrence of hominids and Gigantopithecus at 350 to 200 ka (Wang et al., 2007). Stone tools found at Baise in Guangxi date to 803 +/− 3 ka (Hou et al., 2000). Our own results constrain the occurrence of *Gigantopithecus* in Guangxi to the time range of about 1200 to 300 ka. Taken together, the co-occurrence of *Gigantopithecus* and hominids in Guangxi is dated to between about 800 and 350 ka. This range agrees well with the same co-occurrence in Vietnam at 475 +/− 125 ka. The last known occurrence of *Gigantopithecus* is herein dated by its association at Daxin with the age range of tooth DX3a of 380 and 310 ka, using the coupled ESR/$^{230}$Th/$^{234}$U method (Tables 6 and 7).

Both Wuyun and Upper Pubu are the most recent assemblages among the ones dated in this paper. The Wuyun assemblage dates to the late middle to early late Pleistocene age, based on previous biostratigraphic age estimates, new radiometric data presented by Wang et al. (2007) and our own ESR data. The majority of taxa at Wuyun are either modern or known to persist into the early late Pleistocene (e.g., *Megatapirus augustus*, *Stegodon orientalis*, *Elephas maximus* The EU and LU ages for WY1b of about 215–145 ka provide an age range on *Rhinoceros sinensis* at Wuyun. ESR EU and LU model ages of four specimens of the same taxon from Panxian Dadong cave fall within this time range, while one older age from deep within the Panxian Dadong deposit yielded an older coupled ESR/$^{230}$Th/$^{234}$U age estimate of 296+31/−24 ka (Jones et al., 2004). Panxian Dadong cave is located in western Guizhou Province some 300–400 km to the northwest. The caprid sample (*Capricornus sumatraensis*) (sample WY3a) dates to a time range of about 275 to 175 ka in the Wuyun assemblage. The Upper Pubu samples date to late middle to early late Pleistocene age range based our own data, consistent with biostratigraphic age estimates of the fauna from Lower Pubu cave located 10 m directly below Upper Pubu in the same karst remnant. The Upper Pubu Cave ages presented here are also consistent with our ESR ages at Wuyun Cave, which is located in the same basin less than 2 km away and only 10 m higher in elevation than Upper Pubu Cave. These Upper Pubu Cave ESR ages are also consistent with the Wuyun Cave radiometric ages on flowstones that confine its fossiliferous layers.

Given the historic difficulties of dating materials from Southeast Asia generally and south China in particular, as well as the relatively small number of systematically excavated fossil localities, it is important to begin assigning solid radiometric dates to site assemblages. This helps to refine our understanding of temporal sequences for the region, and it contributes to ongoing debates regarding the validity of the *Ailuropoda–Stegodon* fauna (e.g., Wang et al., 2007), the contributing factors behind Pleistocene megafauna extinctions (e.g., Louys et al., 2007), and paleoenvironmental conditions encountered by hominin populations throughout the region (e.g., Han and Xu, 1989; Dong et al., 2000; Tong, 2001).

## Conclusions

The main outcome of this study is that elements of the *Ailuropoda–Stegodon* fauna have been constrained in time at five different localities. The results agree well with previous estimates for the time range of these sites that placed them into the early, middle and late Pleistocene based on biostratigraphic grounds; however, our results further constrain these age ranges to narrower age ranges in a number of cases. The previous age estimate of early Pleistocene for fauna at Liucheng is now restricted to 1210 to 940 ka, in comparison with 1620 to 780 ka. The previous age estimate for fauna at Daxin of the middle Pleistocene is now restricted to 380 to 310 ka in comparison with a time range of 780 to 130 ka. The Wuming assemblage previously dated to middle Pleistocene (780 to 130 ka) is now restricted to early middle Pleistocene (750 to 480 ka). Biostratigraphic age estimates for Wuyun (middle to late Pleistocene) are confirmed herein. Our Upper Pubu ESR ages of late middle to late Pliestocene are consistent with 1) Wuyun Cave biostratigraphic age estimates, 2) radiometric ages at Wuyun, and 3) the biostratigraphic age estimate of middle to late Pleistocene of Wang et al. (2007) for Lower Pubu Cave that lies just 10 m below Upper Cave in the same karst remnant.

The occurrence of archaic taxa at Liucheng such as *Gomphotherium serridentoides*, *Nestoritherium praesinensis*, *Tapirus peii*, *Rhinoceros chiai*, *Dorcabune liuchengensis*, as well as *Megalovis guangxiensis* and *Cervavitus* (*Cervoceros*) *fenqii*, now have an absolute age estimate of 0.94 to 1.21 Ma, greatly improving previous estimates of early Pleistocene which extends from about 1620 to 780 ka. It also contains early Pleistocene taxa such as *Cuon dubius*, *Hyena licenti*, *Felis teilhardi*, and *Equus yunnanensis* which now can be constrained at that site to 1210 to 940 ka. In addition, the *Gigantopithecus blacki* sample at Liucheng has been shown to be the oldest known in Guangxi.

The increase in size of *Gigantopithecus blacki* teeth found at Wuming and Daxin relative to those found at Liucheng is now constrained in time to have occurred over a time period of about 400,000 yr (from about 1000 ka at Liucheng to about 600 ka at Wuming) Apparent stasis in tooth size is also now constrained to the following 250 ka (from about 600 ka at Wuming to about 350 ka at Daxin). This confirms Zhang's (1985) argument that early Pleistocene to the middle Pleistocene is the timeframe that there is a general increase in tooth size in this species.

At Wuyun, *Megatapirus augustus*, considered as a relatively archaic taxon, occurs after 280 ka indicating it persisted at least to the late middle Pleistocene. Also, archaic *Stegodon orientalis* and modern *Elephas maximus* co-occur at this site, placing these proboscideans into the same timeframe. The dating results from Liucheng and Daxin show the persistence of *Dicoryphochoerus ultimus*, and *Megalovis guangxiensis* from as early as 1200 ka to as late as 300 ka.

The genus *Gigantopithecus* in Guangxi is dated to the time range of about 1200 ka to 300 ka. Taken together with dating evidence from Mohui Cave and Baise, the co-occurrence of

https://doi.org/10.1016/j.yqres.2008.02.008 Published online by Cambridge University Press

*Gigantopithecus* and hominids in Guangxi is dated to between 800 ka and 300 ka. This range spans the same co-occurrence in Vietnam at 475+/−125 ka. The last known occurrence of *Gigantopithecus* is herein dated by its association at Daxin with a tooth dated to between 380 and 310 ka. Though this may not be the age of its final extinction, since, as always, younger occurrences may be found, it is our current best estimate of this.

The cave elevations above the local river level in Table 1 are not correlated directly with age, which was a working hypothesis at the beginning of the study; however, the oldest cave (Liucheng) is indeed one of the two with the highest elevation above the local river.

Overall, application of ESR has shown considerable value in constraining the time range of Pleistocene fauna. Even though the caves had already been previously excavated to a large or complete extent, we were able to overcome the difficulties associated with dating only finds of tooth fragments found in the remaining thin layers of breccia on the cave walls. Future application of the method in similar contexts, at the time of excavation, should yield even better constraints on the time range of species excavated with control for these methods. This would allow for better resolution of the age of individual faunal elements in restricted stratigraphic zones.

## Acknowledgments

WJR and HJ thank the National Sciences and Engineering Council of Canada for financial support, and WW thanks the National History Museum of Guangxi for logistical and financial support, as well as the local cultural ministers in each area for their cooperation and welcoming activities of the field party.

## References

Adamiec, G., Aitken, M.T., 1998. Dose-rate conversion factors: update. Ancient TL 16, 37–50.

Brennan, B.J., Rink, W.J., McGuirl, E.L., Schwarcz, H.P., Prestwich, W.V., 1997. Beta doses in tooth enamel by "One-Group" theory and the ROSY ESR dating software. Radiation Measurements 27, 307–314.

Chen, G., Wang, W., Mo, J., Huang, Z., Tian, F., Huang, W., 2002. Pleistocene vertebrate fauna from Wuyun cave of Taindong county, Guangxi. Vertebrata PalAsiatica 40, 42–51.

Ciochon, R., Olsen, J., James, J., 1990. Other origins: the search for the giant ape in human prehistory. Bantam, New York.

Ciochon, R., Vu The, L., Larick, R., Gonzalez, L., Grün, R., De Vos, J., Yonge, C., Taylor, L., Yoshida, H., Reagan, M., 1996. Dated co-occurrence of Homo erectus and Gigantopithecus from Tham Khuyen Cave, Vietnam. Proceedings of the National Academy of Sciences 93, 3016–3020.

Dong, W., Jin, C., Xu, Q., Liu, J., Tong, H., Zheng, L., 2000. A comparative analysis on the mammalian faunas associated with *Homo erectus* in China. Acta Anthropologica Sinica 19, 246–256.

Gao, J., 1975. Australopithecine teeth associated with *Gigantopithecus*. Vertebrata PalAsiatica 13, 81–88.

Grün, R., Schwarcz, H.P., Chadam, J.M., 1988. ESR dating of tooth enamel: coupled correction for U-uptake and U-series disequilibrium. Nuclear Tracks and Radiation Measurements 14, 237–241.

Guo, S., Shao, Shixiong, 1991. Quaternary lithofacies and palaeogeography in China. In: Zhang,, Z.H., Shao,, S.X. (Eds.), The Quaternary of China. China Ocean Press, Beijing, pp. 122–158.

Han, D., Xu, C., 1985. Pleistocene Mammalian faunas of China. In: Wu,, R., Olsen,, J.W. (Eds.), Paleoanthropology and Paleolithic Archaeology in the People's Republic of China. Academic Press, New York, pp. 267–286.

Han, D., Xu, C., 1989. Quaternary mammalian faunas and environment of fossil humans in south China. In: Wu,, R., Wu,, X., Zhang,, S. (Eds.), Early Humankind in China. Science Press, Beijing, pp. 338–391 (in Chinese).

Hou, M., Potts, R., Yuan, B.Y., Guo, Z.T., Deino, A., Wang, W., Clar, J., Xie, G.M., Huang, W.W., 2000. Mid-Pleistocene Acheulian-like stone technology of the Bose Basin, south China. Science 287, 1622–1626.

Huang, W., 1979. On the age of the cave faunas of South China. Vertebrata PalAsiatica 17, 327–342.

Huang, W., Fang, Q., 1991. Wushan Hominid Site. Ocean Press, Beijing (in Chinese).

Huang, W., Ciochon, R., Gu, Y., Larick, R., Fang, Q., Schwarcz, H., Yonge, C., de Vos, J., Rink, W.J., 1995. Early *Homo* and associated artifacts from Asia. Nature 378, 275–278.

Jones, H.L., Rink, W.J., Schepartz, L.A., Miller-Antonio, S., Huang, W., Ellwood, B.B., 2004. Coupled electron spin resonance (ESR)/uranium-series dating of mammallian tooth enamel at Panxian Dadong, Guizhou Province, China. Journal of Archaeological Science 31, 975–977.

Louys, J., Curnoe, D., Tong, H., 2007. Characteristics of Pleistocene megafauna extinctions in Southeast Asia. Palaeogeograpgy, Palaeoclimatology, Palaeoecology 243, 152–173.

O'Brien, K., Samson, A., Sanna, R., McLaughlin, J.E., 1964. The application of "one group" transport theory to beta-ray dosimetry. Nuclear Science and Engineering 18, 90–96.

Pei, W., 1957. The zoogeographical divisions of Quaternary mammalian faunas in China. Vertebrata PalAsiatica 1, 9–24.

Pei, W., Wu, R., 1956. New materials of *Gigantopithecus* teeth from South China. *Acta* Palaeontologica Sinica 4, 477–490.

Pilbeam, D., 1982. New hominoid skull from the Miocene of Pakistan. Nature 295, 232–234.

Prestwich, W.V., Nunes, J.C., Kwok, C.S., 1997. Beta interface dosimetry in the "one group approximation". Radiation Physics and Chemistry 49, 509–513.

Rink, W.J., 1997. Electron spin resonance (ESR) dating and ESR applications in Quaternary Science and Archaeometry. Radiation Measurements 27, 975–1025.

Rink, W.J., Grün, R., Yalçinkaya, I., Otte, M., Taskiran, H., Valladas, H., Mercier, N., Bar-Yosef, O., Koslowski, J., Schwarcz, H.P., 1994. ESR dating of the last interglacial mousterian at Karaïn Cave, southern Turkey. Journal of Archaeological Science 21, 839–849.

Saegusa, H., 2001. Comparisons of stegodon and elephantid abundances in the Late Pleistocene of southern China. The World of Elephants. International Congress, Rome, pp. 345–349.

Tong, H., 2001. Age profiles of rhino fauna from the Middle Pleistocene Nanjing man site, south China — explained by the rhino specimens of living species. International Journal of Osteoarchaeology 11, 231–237.

Tong, H., 2005. Dental characters of the Quaternary tapirs in China, their significance in classification and phylogenetic assessment. Geobios 38, 139–150.

Tong, H., 2006. Composition des faunes de mammiféres quaternaries en Chine selon un gradient Nord–Sud. L'Anthropologie 110, 870–887.

Tong, H., 2007. Occurrences of warm-adapted mammals in north China over the Quaternary Period and their paleo-environmental significance. Science in China Series D: Earth Sciences 50, 1327–1340.

Wang, W., Potts, R., Hou, Y., Chen, Y., Wu, H., Yuan, B., Huang, W., 2005. Early Pleistocene hominid teeth recovered in Mohui cave in Bubing Basin, Guangxi, South China. Chinese Science Bulletin 50, 2777–2782.

Wang, W., Potts, R., Yuan, B., Huang, W., Cheng, H., Edwards, R.L., Ditchfield, P., 2007. Sequence of mammalian fossils, including hominoid teeth, from the Bubing Basin caves, South China. Journal of Human Evolution 52, 370–379.

Wu, R., Lin, S., 1985. Chinese Paleoanthropology: retrospect and prospect. In: Wu, R., Olsen, J.W. (Eds.), Paleoanthropology and Paleolithic Archaeology in the People's Republic of China New York. Academic Press, pp. 1–27.

Xue, X., Zhang, Y., 1991. Quaternary mammalian fossils and fossil human being. In: Zhang, Z.H., Shao, S.X. (Eds.), The Quaternary of China. China Ocean Press, Beijing, pp. 307–374.

Zhang, Y., 1985. *Gigantopithecus* and "*Australopithecus*" in China. In: Wu,, R., Olsen,, J.W. (Eds.), Paleoanthropology and Paleolithic Archaeology in the People's Republic of China. Academic Press, New York, pp. 69–78.

Zhou, M., 1957. Mammalian faunas and the correlation of Tertiary and early Pleistocene of South China. Kexue Tongbao 13, 394–399.